# Electromagnetic liquid pistons for capillarity-based pumping†

**Bernard A. Malouin Jr,[a] Michael J. Vogel,[b] Joseph D. Olles,[a] Lili Cheng‡[a] and Amir H. Hirsa*[a]**

***Received 10th September 2010, Accepted 5th November 2010***
**DOI: 10.1039/c0lc00397b**

The small scales associated with lab-on-a-chip technologies lend themselves well to capillarity-dominated phenomena. We demonstrate a new capillarity-dominated system where two adjoining ferrofluid droplets can behave as an electronically-controlled oscillator or switch by an appropriate balance of magnetic, capillary, and inertial forces. Their oscillatory motion can be exploited to displace a surrounding liquid (akin to an axial piston pump), forming electromagnetic "liquid pistons." Such ferrofluid pistons can pump a precise volume of liquid *via* finely tunable amplitudes (*cf.* pump stroke) or resonant frequencies (*cf.* pump speed) with no solid moving parts for long-term operation without wear in a small device. Furthermore, the rapid propagation of electromagnetic fields and the favorable scaling of capillary forces with size permit micron sized devices with very fast operating speeds (~kHz). The pumping dynamics and performance of these liquid pistons is explored, with experimental measurements showing good agreement with a spherical cap model. While these liquid pistons may find numerous applications in micro- and mesoscale fluidic devices (*e.g.*, remotely activated drug delivery), here we demonstrate the use of these liquid pistons in capillarity-dominated systems for chip-level, fast-acting adaptive liquid lenses with nearly perfect spherical interfaces.

## Introduction

A central thrust in micro total analysis systems (μTAS) is the intense search for highly integrable liquid pumping technologies, with applications ranging from separations and drug dosing to genomics and proteomics.[1–5] At smaller scales, surface-to-volume ratios become large, diffusion times of reactants become small, and the forces associated with surface tension become powerful enough to play a vital role.[6,7] It is possible to scale mechanical pumps to sizes suitable for lab-on-a-chip applications, but these systems can become quite complex with considerable fabrication and integration challenges involving microscale bearings, rotors, and valves.[5] These limitations in conventional pumping technologies have spawned a need for innovative, non-traditional strategies.

Several strategies for fluidic pumps with no solid moving parts have been introduced in the literature, each with a unique set of advantages and limitations. For example, passive approaches like capillary pumps require very little power but are highly sensitive to the fluid used and lack easy tunability.[7,8] More active approaches like electroosmosis and electrowetting scale quite well[9] but can be highly dependent on the pumped liquid's physical properties (*e.g.*, zeta potential, surface tension and contact angles), limiting device universality.[4,10] Here, at the nexus of electromagnetics and capillarity-dominated fluid dynamics, we present a new strategy for micro- and mesoscale liquid pumping by means of electromagnetic liquid pistons. Akin to solid pistons found in axial pumps, these liquid pistons are capable of precisely pumping a surrounding liquid by means of finely tunable amplitudes (*cf*, piston stroke) and resonant frequencies (*cf*, piston speed), all the while with no wear, easy device integration, and a range of liquids capable of being pumped.

The system features a coupled ferrofluid droplet immersed in water. In the presence of an oscillating magnetic field (AC voltage) the coupled ferrofluid droplet system becomes a liquid resonator, capable of moving the surrounding liquid back-and-forth from one chamber to another. Alternatively, for applications requiring a positive displacement pump, the device can be operated as an array of bistable liquid switches activated by short DC voltage pulses. We present measurements and a model for the behavior of these liquid pistons. Additionally, the ferrofluid liquid pistons can be adapted for a multitude of practical lab-on-a-chip applications including drug delivery, dosing, PCR thermal cycling, and other emerging fields such as adaptive lenses. In adaptive optics, where, by further utilizing the propensity of interfacial tension to favor highly spherical shapes, liquid lenses can be formed that are smooth on the molecular level.[11,12] Actuation of these adaptive lenses by liquid pistons enables systems that are compact and highly integrable for true lab-on-a-chip functionality.

## Liquid piston oscillators

### Device description

At appropriate length scales, the forces associated with surface tension dominate over gravity producing interesting phenomena as in the case of liquid adhesion microdevices,[9,13] liquid switches,[13,14] and liquid oscillators.[15,16] In the latter, natural oscillators consisting of liquid droplets in air have been shown to maintain spherical interfaces due to surface tension while resonating at frequencies in excess of 100 Hz.[17] Meanwhile, liquid switches have been demonstrated, with switching times of a few

[a]*Department of Mechanical, Aerospace, and Nuclear Engineering, Rensselaer Polytechnic Institute, Troy, NY, 12180. E-mail: hirsaa@rpi.edu.*
[b]*Independent Researcher, Voorhees, NJ, 08043*

† Electronic supplementary information (ESI) available: Supplemental Movie 1 and 2. See DOI: 10.1039/c0lc00397b

‡ Current address: GE Global Research, Niskayuna, NY 12309.

microseconds possible for scaled down devices.[13] Previous studies have nearly exclusively utilized water surrounded by air, in part due to its large and well-characterized surface tension and wetting properties. Here, a new system is introduced, replacing the surrounding air with a liquid that can be effectively pumped due to the motion of the oscillating droplet. The concept of ferrofluid liquid pistons pumping a second droplet between two chambers is illustrated in Fig. 1a and 1b. Two holes are drilled or etched into a substrate. One hole is overfilled with an oil-based ferrofluid (a colloidal suspension of magnetic particles in an oil carrier fluid) so that a certain volume of liquid protrudes from both sides of the substrate. The contact lines of the droplets are fixed by geometry and surface chemistry at the perimeter of the hole in the substrate. The second hole can be left as a conduit to pump the surrounding liquid between chambers or, as explored here, overfilled with another liquid to the desired volume (*e.g.*, to form a liquid lens or a droplet of solution to be cycled between two baths as in PCR[3]). The rest of the system is filled with an immersion liquid (water in this case) that is immiscible with the two sets of coupled droplets.

In practice, the maximum size of the droplets is dictated by the relative balance of capillary forces to gravitational body forces.[18] This maximum size is given by the capillary length $\lambda = \sqrt{\gamma/|\rho_D - \rho_S|g}$, with $\gamma$ the interfacial tension, $\rho_D$ and $\rho_S$ the density of the droplet and surrounding liquid, respectively, and $g$ the acceleration due to gravity. In typical air/water systems (where $\rho_S$ is negligibly small) this capillary length is around 1 mm; however, for ferrofluids and various other oils surrounded by water this capillary length has significant latitude, permitting systems from hundreds of nanometres to centimetres. The experimental system is sealed in an enclosure while the 1.5 mm thick substrate serves to separate the two different chambers (*e.g.*, one on top, one on bottom) with the only connection between them being the two sets of immiscible droplets. It is now straightforward to see how an oscillation of the liquid piston would cause an opposite phase, but identical volume displacement, oscillation in the other droplet.

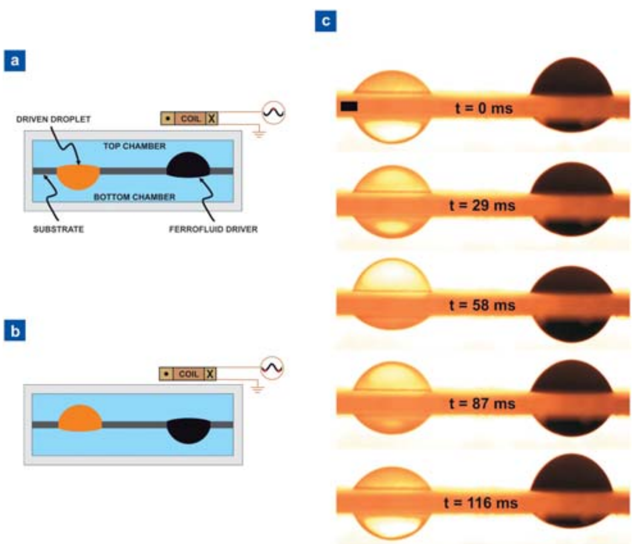


**Fig. 1** Electromagnetic liquid pistons for capillarity-based pumping. (a,b) Two holes are made in a substrate. One hole is overfilled with ferrofluid (right, black) to form an electromagnetically activated liquid piston. The second hole can be left unfilled as a connection between chambers or, as shown here, filled with another droplet for PCR or liquid lens applications. The system is surrounded by water (blue) and sealed. An electromagnet is given a sinusoidal signal to drive the resonating liquid piston. Due to the incompressibility of the surrounding liquid, a displacement in the liquid piston causes an opposite phase but equal volume displacement in the other droplet. This results in a pumping of the liquid back-and-forth between two liquid baths. (c) Time series of images of liquid pistons driving the oscillation of another (transparent, silicone oil) droplet at a resonance of 8.6 Hz. Scale bar is 1 mm.

To create the oscillations of the liquid piston, an electromagnetic coil[19] is positioned above the ferrofluid but external to the liquid chamber. A sinusoidal signal is supplied to the coil (amplitude of 3 volts), creating an oscillating non-uniform magnetic field in the vicinity of the droplet interface[20,21] which produces oscillatory motion of the liquid piston. This is due to the magnetic force (per unit volume), $F$, on the ferrofluid given by[22,23]

$$F = \mu_o\, M \cdot \nabla H + \frac{1}{2}\mu_o\, \nabla \times (M \times H) \qquad (1)$$

where $\mu_o$ is the permeability of free space, $M$ is the magnetization of the material, and $H$ is the magnetic field strength. The first term on the right side of eqn (1) is the dominant term, called the magnetic Kelvin force,[22] with the second term representing torque contributions when the magnetization and field vectors are not collinear,[23] as may be the case for a continually oscillating field. Due to the proportionality with both the local field (through $M$) and field gradient, the resulting force provides only an attractive force (*i.e.*, a "pull"), regardless of the polarity of the applied voltage on the electromagnet. For simplicity, a single electromagnet is used to perturb the liquid piston driver, with spring-like capillarity the restoring force. Dynamically, this is reminiscent of a mass-spring system with liquid inertia acting as the mass, capillarity acting as the spring, and the magnetic force providing the forcing function. The system then oscillates between two extreme positions, depicted by Fig. 1a (maximum height) and 1b (minimum height).

In the existing device, the triple contact line (liquid/liquid/solid) is fixed at the perimeter of the hole in the substrate. These pinned contact lines are essential features as they eliminate dissipation associated with advancing and receding contact lines.[14,24] Moreover, the overall efficiency of the device is enhanced by driving it at the system resonance. At resonance, capillarity and inertia are finely balanced to provide maximum amplitude oscillations with minimal forcing of the system. The system oscillating at resonance is shown in the snapshots of Fig. 1c. In this setup, a 5 mm diameter transparent droplet is shown on the left (silicone oil) driven by a 5 mm ferrofluid liquid piston driver (EMG 909, Ferrotec Corp., appears black), drilled into a 1.5 mm thick Delrin substrate. The entire system depicted, including surrounding water (transparent), resonates at 8.6 Hz as it pumps the surrounding water at 6.5 µL per oscillation (also available as Supplemental Movie 1†).

## Dynamics

Two of the principal characteristics of the electromagnetic liquid pistons are the amplitude and frequency. The amplitude dictates how much liquid will be displaced (or pumped) per oscillation.

 

Meanwhile, the speed of the pumping mechanism is greatly dependent on the system's natural frequency. Major factors in the resonant frequency of the system are the capillary forces due to each of coupled droplets in the system. To increase resonant frequencies, therefore, the capillary force must be amplified. One such way to accomplish this is to decrease the hole size, leading to a device whose frequency response scales favorably with reduced size. To this end, utilizing parallel actuation *via* arrays of smaller coupled droplets (to maintain the necessary total displacement of the driver droplets) becomes a viable strategy.

To investigate the dynamic response of the system with parallel actuation, three configurations using arrays of smaller liquid piston drivers were created and tested, as depicted in Fig. 2. For these cases, the driven droplets (1-methylnaphthalene, useful for liquid lenses) overfilled a hole of diameter 5 mm to a non-dimensional volume $v/v_{sph} = 0.5$, where $V_{sph}$ is the volume of a sphere with the same diameter as the orifice. The liquid piston driver array is then varied with cases including one 5 mm driver ($N = 1$), an array of three 3 mm drivers ($N = 3$), and an array of seven 2.5 mm drivers ($N = 7$), as shown in Fig. 2a.

The inset in Fig. 2b shows the experimentally measured frequency response (normalized by maximum amplitude for each case) of the three configurations, given a sinusoidal input to the electromagnet. Actuating with arrays of smaller drivers is demonstrated to increase the response of the system. The resonance measurements show good agreement with a nonlinear model of the system, assuming spherical cap droplets (Fig. 2b). This model is the result of a force balance on the liquid droplet system. The details of the full theoretical approach for the nonlinear model will be presented elsewhere, but the following simplified version (linearized, assuming density matched liquids, and equal interfacial tensions) may be useful for some readers. This prediction for system resonant frequency, $\omega_{res}$, is:

$$\omega_{res}{}^{2} \approx \frac{4\gamma}{\pi^{2}\rho\, L_{tot}} \left(\frac{1}{R_L{}^{2}} + \frac{1}{R_D{}^{2}}\right) \left(1 - \frac{V}{V_{sph}}\right) \qquad (2)$$

where $\rho = \rho_D = \rho_S$, $R_L$ and $R_D$ are the hole radii for the lens and liquid piston driver, respectively, and $L_{tot}$ is the total path length (twice the sum of substrate thickness and hole-to-hole spacing). Note that $\omega_{res}$ depends only on the size of the liquid piston drivers in the array, where the number of drivers dictates the total volume displacement.

The favorable scaling of such systems to micron-sized devices reveals the true potential of liquid piston pumps for lab-on-a-chip applications. Table 1 shows how the performance is expected to scale with device size, yielding micron-sized liquid pistons resonating at several hundred kilohertz.[25] While a single piston yields precise displacements on the order femtolitres, a device that consists of droplet arrays (covering a fixed planform area of only 20 mm$^2$) operating in unison can offer higher throughputs, on the order of nanolitres with high surface-to-volume ratios.

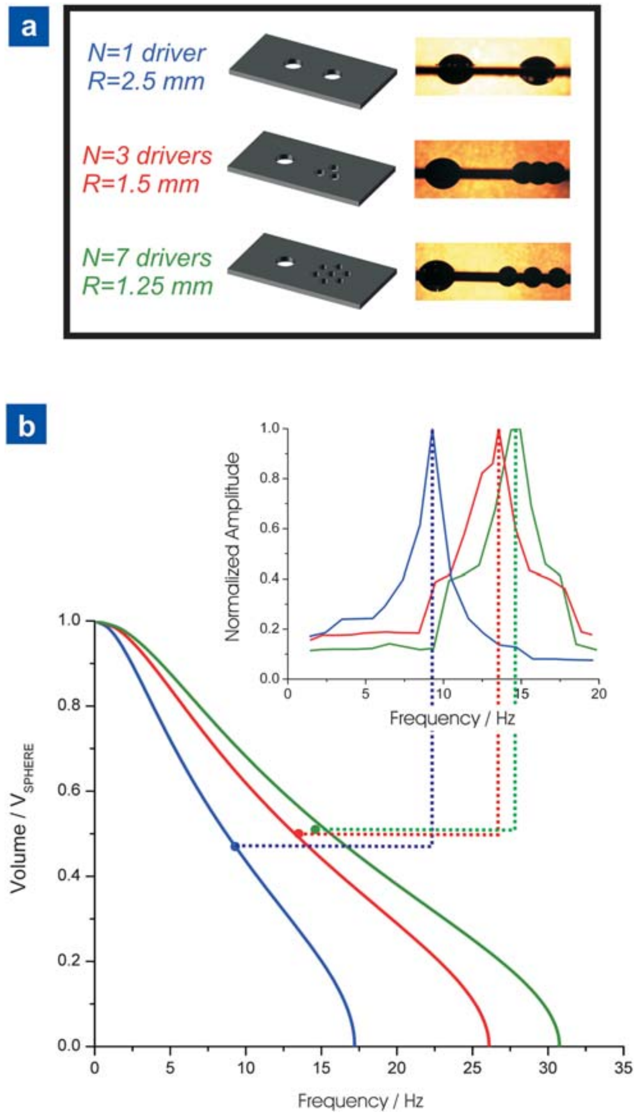


**Fig. 2** Dynamics of liquid piston driver arrays for parallel actuation. Arrays of smaller drivers increase the frequency response of the liquid piston pump system. (a) Shows three configurations with the same 5 mm driven droplet and different arrays of smaller ferrofluid liquid pistons. The baseline ($N = 1$) case has one 5 mm driver, the $N = 3$ case features an array of three 3 mm drivers, and the $N = 7$ case corresponds to an array of seven 2.5 mm drivers. The inset of (b) shows the experimentally measured frequency response of each configuration, with the maximum amplitude of each normalized to unity. Significantly higher resonance frequencies are observed using arrays of smaller drivers. (b) Shows good agreement between experiment and a spherical cap model for the three liquid resonating system.

## Applications

Electromagnetic liquid pistons may find immediate use as small volume pumps with no moving parts to eliminate wear in microfluidic transport for use in mixing, injection, and separations.[4] However, surface tension bestows such systems with an additional feature – nearly perfect spherical interfaces.[11] This attribute makes the oscillating droplet an effective lens.[17,26,27] Furthermore, as the coupled droplets oscillate, the curvature of the interface continually changes, giving rise to a variable focal length liquid lens immune to evaporation and essentially invariant to orientation as gravitational effects are minimized relative to surface tension by keeping the gravitational Bond number, $Bo \equiv |(\rho_D - \rho_S)\, g\, R^2/\gamma|$, less than unity.[28] Fig. 3a demonstrates the variable focal length ability of the system,

**Table 1** Scaling of liquid piston systems, single pistons and arrays

| | | Volume displaced per oscillation | |
|---|---|---|---|
| Hole radius | Frequency | Single drop | Many drops, fixed area |
| 2.5 mm | 8.8 Hz | 6.5 μL | 6.5 μL ($N = 1$) |
| 250 μm | 280 Hz | 6.5 nL | 650 nL ($N = 100$) |
| 25 μm | 8.8 kHz | 6.5 pL | 65 nL ($N = 10^4$) |
| 2.5 μm | 280 kHz | 6.5 fL | 6.5 nL ($N = 10^6$) |

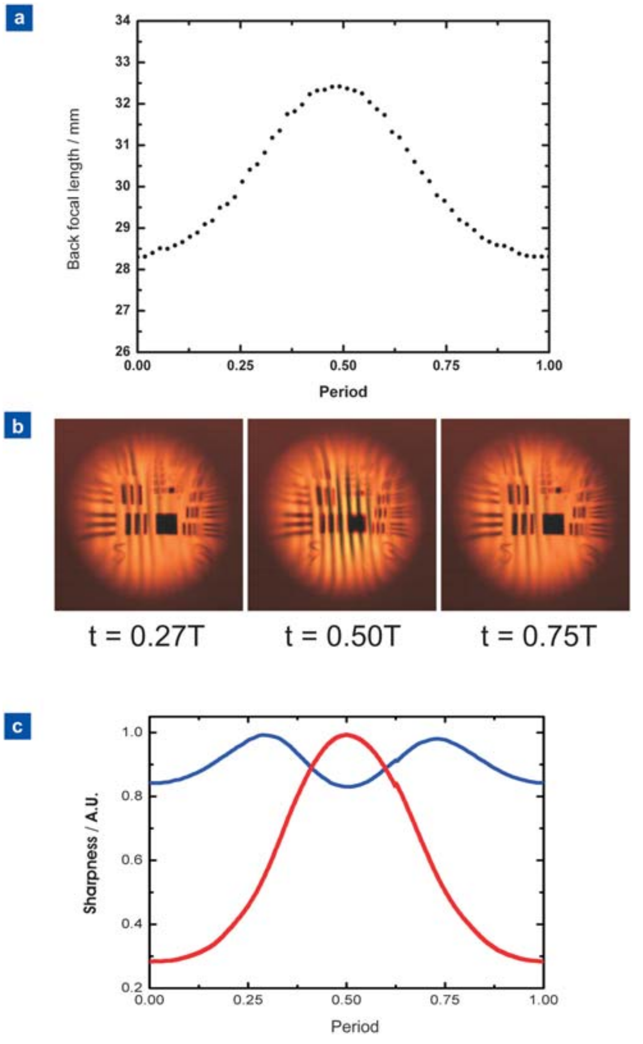


**Fig. 3** Application of liquid pistons to actuate liquid lenses. The oscillatory pumping of the liquid pistons creates an out-of-phase, oscillatory displacement in the (transparent) driven droplet. This causes the curvature of the driven droplet (and therefore focal length) to continually change leading to a variable focal length liquid lens (a) where a range of imaging planes is scanned during each oscillation. (b) Shows images of two targets through a 5 mm diameter oscillating liquid lens driven by liquid pistons. A Ronchi grating (vertical lines) is placed 10 mm above the lens, with a US Air Force resolution target (pattern of tick marks) 3 mm above that. As the system oscillates, each of these targets comes into focus at different points in the period. (c) Shows the sharpness (focus) of each target determined over one period (red points are Ronchi grating, blue points are AF target).

where the back focal length has been determined from an edge detection algorithm and plotted over one cycle of oscillation.[29]

To further illustrate the implications of the variable focal length capabilities, two targets are imaged through the oscillating liquid lens by a high speed camera.[30] In Fig. 3b, a Ronchi grating (series of vertical lines) is placed above the oscillating lens droplets. A resolution target (pattern of small tick marks) is then placed above the Ronchi grating. During each oscillation of the system (of period T), a range of imaging planes is scanned, producing a sharp image of each target, as shown in Fig. 3b (also available as Supplemental Movie 2†). In Fig. 3c the sharpness of each target has been analyzed,[31] where the relative sharpness is seen to be at a maximum (greatest focus) at different times in the oscillation for each target.

## Liquid piston switches

### Description

While results up to this point have been obtained using harmonically-driven electromagnetic liquid pistons of volumes $v/v_{sph} < 1$, a very different behavior emerges for systems with liquid pistons of larger volume, $v/v_{sph} > 1$. Due to the minimization of surface energy of large coupled droplets, a bifurcation occurs in the energy landscape,[9,14] yielding two stable configurations for the ferrofluid liquid switches.[32] That is, a droplet with more volume on the bottom can be toggled such that more volume now rests on the top, where it is again stable. Fig. 4a illustrates this concept where larger volume liquid pistons (right) are initially in a stable state. A small DC pulse is applied to the electromagnet and a ferrofluid switch is toggled from a bottom-heavy state to a top-heavy state.

The shift in volume produced by toggling a given number of ferrofluid switches displaces an equal volume of surrounding liquid. In this regard, discrete volumes of liquid can be pumped with a positive displacement from one chamber to the other. This is shown in the plot of Fig. 4b, where different liquid switches are toggled to pump precise microlitre volumes. Such an on-demand, small volume dispenser may be especially useful for biomedical dosing, where implantable devices could be activated remotely to provide precise doses of drugs *in situ*. Also note that since the switches are bistable, once they have been toggled, no additional power to the electromagnet is necessary to maintain the new state (equilibrium), making for an energy efficient device.

Returning once again to the application of adaptive lenses, Fig. 4b also demonstrates how the measured focal length of the driven lens droplet can be finely tuned by toggling a given number of ferrofluid liquid switches. This type of configuration closely mimics the function of an optometrist's phoropter, replacing various solid lenses of differing optical power with a single, reconfigurable liquid lens in a compact, lightweight device. Possible applications for such energy efficient, reconfigurable liquid lenses may include medical imaging, where adaptive components to surgical tools may be of great utility to practitioners inspecting the highly irregular topology of internal tissues.

## Conclusion

This work has introduced the use of electromagnetically-controlled liquid pistons that offer favorable performance with

 

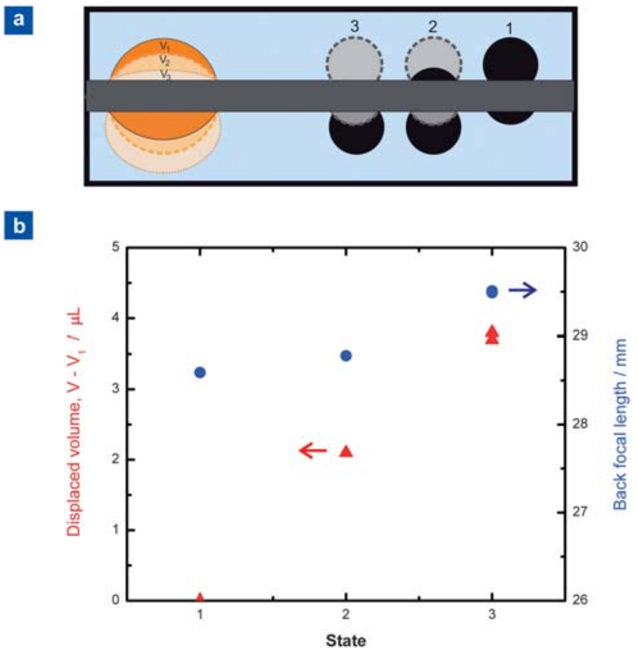


**Fig. 4** Addressable liquid pistons for discrete, remotely activated pumping. Larger volume droplets ($v/v_{sph} > 1$) become bistable liquid switches that can be toggled with only momentary electromagnetic pulses. (a) Stable droplets of ferrofluid with more volume initially on the bottom can be toggled such that more volume now rests on top (where they are again stable) using only a brief DC pulse. The volume pumped can be carefully controlled by the number of liquid switches being toggled (three are shown in this schematic). (b) Different numbers of ferrofluid liquid switches are toggled and the volume displaced in the pumped droplet is determined. Moreover, this displaced liquid produces a change in the curvature of the pumped droplet (liquid lens). By toggling different numbers of ferrofluid liquid switches, the liquid lens can be reconfigured for different static focal lengths (b). As the liquid switches are bistable, once toggled no additional power is needed by the electromagnet.

reduced size. These liquid pistons can be driven with only a few volts and are highly integrable into meso- and microfluidic devices. Furthermore, these liquid pistons can be used to pump liquid back-and-forth between two chambers, or to drive the oscillation of another droplet of solution between two distinct baths (*e.g.*, different temperatures or reagents) for versatile lab-on-a-chip applications. The latter can also be exploited by connecting the chambers with an optical liquid forming a liquid lens system. By balancing liquid inertia against capillarity, these scalable liquid lens systems become fast-acting adaptive lenses with variable focal lengths. Moreover, by utilizing an array of bistable capillary switches as ferrofluid drivers, energy efficient reconfigurable lenses become possible as well as other potential applications including positive displacement pumps with discrete steps for biomedical dosing and drug delivery.

## Acknowledgements

The authors wish to thank Sheppard J. Salon and Gerald P. Selvaggi for many useful discussions on electromagnetism and for some of the electrical equipment. Deborah Furey is also thanked for insightful discussions on switch functionality. This work was supported by DARPA Grant No. HR0011-09-1-0052.

## References and Notes

1 P. S. Dittrich and A. Manz, *Nat. Rev. Drug Discovery*, 2006, **5**, 210–218.
2 S. Z. Razzacki, P. K. Thwar, M. Yang, V. M. Ugaz and M. A. Burns, *Adv. Drug Delivery Rev.*, 2004, **56**, 185–198.
3 B. H. Weigl, R. L. Bardell and C. R. Cabrera, *Adv. Drug Delivery Rev.*, 2003, **55**, 349–377.
4 J. Xie, J. Shih, Q. Lin, B. Yang and Y.-C. Tai, *Lab Chip*, 2004, **4**, 495–501.
5 F. Amirouche, Y. Zhou and T. Johnson, *Microsyst. Technol.*, 2009, **15**, 647–666.
6 Y. Pomeau and E. Villermaux, *Phys. Today*, 2006, **59**, 39–44.
7 M. Zimmermann, H. Schmid, P. Hunziker and E. Delamarche, *Lab Chip*, 2007, **7**, 119–125.
8 G. M. Walker and D. J. Beebe, *Lab Chip*, 2002, **2**, 131–134.
9 M. J. Vogel, P. Ehrhard and P. H. Steen, *Proc. Natl. Acad. Sci. U. S. A.*, 2005, **102**, 11974–11979.
10 L. X. Chen, J. P. Ma, F. Tan and Y. F. Guan, *Sens. Actuators, B*, 2003, **88**, 260–265.
11 A. W. Adamson, *Physical Chemistry of Surfaces*, Wiley, New York, 1990.
12 D. Graham-Rowe, *Nat. Photonics*, 2006, 2–4, sample.
13 M. J. Vogel and P. H. Steen, *Proc. Natl. Acad. Sci. U. S. A.*, 2010, **107**, 3377–3381.
14 A. H. Hirsa, C. A. López, M. A. Laytin, M. J. Vogel and P. H. Steen, *Appl. Phys. Lett.*, 2005, **86**, 014106.
15 E. A. Theisen, M. J. Vogel, C. A. López, A. H. Hirsa and P. H. Steen, *J. Fluid Mech.*, 2007, **580**, 495–505.
16 S. Ramalingam and O. A. Basaran, *Phys. Fluids*, 2010, **22**, 112111.
17 C. A. López and A. H. Hirsa, *Nat. Photonics*, 2008, **2**, 610–613.
18 Other factors including wetting and pinning properties can also impose limits on maximum size if not carefully addressed.
19 An electromagnet, placed outside the liquid-filled chambers, was used to drive the system. The centimetre scale electromagnet required a 3 volt signal. The present system can be further scaled down with high permeability alloys and coils integrated into the plate, reducing physical dimensions, current requirements, or both by at least an order of magnitude.
20 F. K. Wohlhuter and O. A. Basaran, *J. Fluid Mech.*, 1992, **235**, 481–510.
21 S. Afkhami, Y. Renardy, M. Renardy, J. S. Riffle and T. St. Pierre, *J. Fluid Mech.*, 2008, **610**, 363–380.
22 R. E. Rosensweig. *Ferrohydrodynamics*. Dover, New York, 1985, pp. 100–123.
23 S. Odenbach. *Ferrofluids: Magnetically Controllable Fluids and Their Applications*, Springer, Heidelberg, 2002, pp. 62–79.
24 L. M. Hocking, *J. Fluid Mech.*, 1987, **179**, 253–266.
25 Scaling of the system is done with the nonlinear model developed (simplified for eqn (2)). Note that it should be possible to keep the magnetic Bond number, $Bo_m \equiv \mu_0 H_0^2 R/\gamma$ where $H_0$ is the applied magnetic field strength, constant over this range of device sizes.
26 S. Kuiper and B. H. W. Hendriks, *Appl. Phys. Lett.*, 2004, **85**, 1128–1130.
27 It is noteworthy that even if the magnetic field is sufficiently strong to distort the liquid piston (here, magnetic Bond number, $Bo_m \approx 0.55$), interfacial tension can preserve the spherical geometry in the liquid lens.
28 A.H. Hirsa, B.A. Malouin, M.J. Vogel, L. Cheng and J.D. Olles, US Provisional Patent Appl. #61/368,020, filed 27 July 2010.
29 C. A. López, C.-C. Lee and A. H. Hirsa, *Appl. Phys. Lett.*, 2005, **87**, 134102.
30 A Redlake HS2-C high speed camera is utilized, operated at 1500 frames per second. A 135 mm Nikkor Telephoto lens on a bellows is also used in the optical train.
31 For each pixel the sharpness is the average magnitude of the difference in intensities between a pixel and its neighboring pixels. As edges and textures come into focus, maximum contrast between neighboring pixels is expected.
32 B. A. Malouin, M. J. Vogel and A. H. Hirsa, *Appl. Phys. Lett.*, 2010, **96**, 214104.